Biochemical and Pre-Steady-State Kinetic Characterization of the Hepatitis C Virus RNA Polymerase (NS5BΔ21, HC-J4)[†]

Janina Cramer,[#] Joachim Jaeger,[‡] and Tobias Restle*[,§]

Max-Planck-Institut für Molekulare Physiologie, Abteilung Physikalische Biochemie, Otto-Hahn-Strasse 11, 44227 Dortmund, Germany, Wadsworth Center, New York State Department of Health, Center for Medical Science, 150 New Scotland Avenue, Albany, New York 12208, and Universitätsklinikum Schleswig-Holstein, Campus Lübeck, Institut für Molekulare Medizin, Ratzeburger Allee 160, 23538 Lübeck, Germany

Received July 27, 2005; Revised Manuscript Received November 16, 2005

ABSTRACT: Here we report a detailed characterization of the biochemical and kinetic properties of the hepatitis C virus (HCV, genotype-1b, J4 consensus) RNA-dependent RNA polymerase NS5B, by performing comprehensive RNA binding, nucleotide incorporation, and protein/protein oligomerization studies. By applying equilibrium fluorescence titrations, we determined a surprisingly high dissociation constant (K_d) of approximately 250 nM for single-stranded as well as for partially double-stranded RNA. A detailed analysis of the nucleic acid binding mechanism using pre-steady-state techniques revealed the association reaction to be nearly diffusion controlled. It occurs in a single step with a second-order rate constant (k_{on}) of 0.273 $nM^{-1}\ s^{-1}$. The dissociation of the nucleic acid−polymerase complex is fast with a dissociation rate constant (k_{off}) of 59.3 s^{-1}. With short, partially double-stranded RNAs, no nucleotide incorporation could be observed, while de novo RNA synthesis with short RNA templates showed nucleotide incorporation and end-to-end template switching events. Single-turnover, single-nucleotide incorporation studies (representing here the initiation and not processive polymerization) using dinucleotide primers revealed a very slow incorporation rate (k_{pol}) of 0.0007 s^{-1} and a K_d of the binary enzyme−nucleic acid complex for the incoming ATP of 27.7 μM. Using dynamic laser light scattering, it could be shown for the first time that oligomerization of HCV NS5B is a dynamic and monovalent salt concentration dependent process. While NS5B is highly oligomeric at low salt concentrations, monomers were only observed at NaCl concentrations above 300 mM. Binding of short RNA substrates led to a further increase in oligomerization, whereas GTP did not show any effect on protein/protein interactions. Furthermore, nucleotide incorporation studies indicate the oligomerization state does not correlate with enzymatic activities as previously proposed.

The World Health Organization has estimated about 3% of the world's human population to be infected with the hepatitis C virus (HCV)[1] (*1*). In most HCV carriers, the initial infection develops into a chronic hepatitis which eventually leads to cirrhosis and hepatocellular carcinoma (*2*). Chronic HCV infections are now the leading indication for liver replacement surgery in the developed world. There is currently no vaccine against HCV, and the available therapies are expensive, poorly tolerated, and have limited success rates as they are not generally effective against all clinically relevant HCV genotypes. Clearly, there is an urgent need for the development of better strategies to block viral replication. One promising approach is the inhibition of the viral RNA-dependent RNA polymerase (RdRp) NS5B, which is the core enzyme of the HCV replicase complex.

Prerequisite for the rational design of such inhibitors is a profound knowledge of the target protein in combination with appropriate biochemical test systems and suitable crystal forms for structural studies on inhibitor complexes. Although numerous reports concerned with the biochemical properties of this viral polymerase have been published, many aspects about the detailed mechanism of action remain obscure. This problem can be in part attributed to the fact that the HCV polymerase has been shown to fulfill its task as part of a membrane-associated multiprotein complex, a situation not necessarily resembled by in vitro studies using recombinant protein. In terms of structural characterization, the situation is much more encouraging. Several X-ray structures of this enzyme from various HCV isolates and genotypes have been solved independently. The most thoroughly studied form of HCV RdRP is based on the consensus sequence of the HC-BK isolate (*3*−*6*). Another, recently reported structure is derived from the HC-J4 isolate (*7*) showing differences in crystal form and biochemical characteristics (*8*). The enzyme reveals a right-handed structure with domains representing fingers, palm, and thumb as described for other polymerases. Interestingly, there is an intensive interaction between the fingers and the thumb domains leading to a fully encircled

[†] This work has been supported by EC Grant No. QLK2-CT-2001-01451.

* To whom correspondence should be addressed: Tel. +49 451 500 2745. Fax +49 451 500 2729. E-mail: restle@imm.uni-luebeck.de.

[#] Max-Planck-Institut für Molekulare Physiologie.

[‡] New York State Department of Health.

[§] Universitätsklinikum Schleswig-Holstein.

[1] Abbreviations: HCV, hepatitis C virus; NS5B, nonstructural protein 5B; RdRp, RNA-dependent RNA polymerase; p/t, primer/template; NTA, nitrilo triacetic acid; nt, nucleotides; ds, double stranded; PAGE, polyacrylamide gel electrophoresis.

10.1021/bi051483s CCC: $33.50
Published on Web 02/28/2006

active site cavity. This unusual closed structure has also been described for many other closely and distantly related viral RNA polymerases: bovine viral diarrhea virus (BVDV) NS5B (*9*), bacteriophage ϕ6 polymerase (*10*), reovirus lambda3 protein (*11*), and foot-and-mouth disease virus 3D polymerase (*12*). A novel structural motif of HCV NS5B is a β-hairpin extending from the thumb domain into the active site cleft. This motif has been proposed to represent a steric barrier for the binding of partially double-stranded nucleic acid substrates (*5*). A possible function of this β-hairpin, conserved in all flaviviridae polymerases, might be proper positioning of the 3′-end of the bound RNA for effective initiation of RNA synthesis (*5*, *13*). In this context, the flexible C-terminus of the polymerase has been proposed to be involved in the regulation of the initiation process (*14*−*16*). Initiation of RNA synthesis in vitro by the HCV polymerase may occur via different mechanisms. It has been reported NS5B can utilize short RNA primers to start RNA synthesis (*13*, *17*−*20*). Furthermore, it has been shown that the enzyme is also capable of initiating RNA synthesis in the absence of any RNA primer performing copy back and/or de novo synthesis (*19*, *21*−*25*). However, in general NS5B displays low template binding specificity and has been reported to utilize structured and unstructured RNA from different sources as substrate for the initiation of RNA synthesis (*13*, *17*, *18*, *21*, *22*, *26*−*28*).

Several biochemical studies of viral RdRps and reverse transcriptases indicate that dimerization and/or oligomerization are critical concerning the enzymatic properties of those enzymes (*29*−*33*). In this context, it has been reported that HCV NS5B shows a tendency to oligomerize and suggested that this oligomerization regulates the polymerase activity (*34*−*36*).

In this study, we present the first comprehensive biochemical characterization of HC-J4 NS5BΔ21, a C-terminally truncated polymerase based on the consensus sequence of pCV-J4L6S. Steady-state and pre-steady-state kinetic analyses were performed aiming to unravel mechanistic details of RNA binding and nucleotide incorporation catalyzed by this viral RdRp. Using dinucleotide primers, we have established a nucleotide incorporation assay suitable of deriving quantitative data on the polymerase reaction pathway. Furthermore, we present experimental evidence regarding the controversially discussed issue of oligomerization of HCV RNA polymerase and possible implications of this phenomenon on in vitro studies of this fascinating and pharmaceutically relevant enzyme.

EXPERIMENTAL PROCEDURES

Protein. NS5BΔ21 (derived from the HC-J4 isolate) (*7*) was expressed in the *Escherichia coli* strain BL21(DE3). Cells were grown at 30 °C in 10 L LB media, induced at an OD_{600} of 0.7 by adding 0.4 mM IPTG and harvested after 4 h at 25 °C. Cells were resuspended in buffer A (100 mM Tris/HCl pH 8.0, 300 mM NaCl, 10 mM $MgCl_2$, 0.1% Triton X-100 and 10 mM β-mercaptoethanol) and lyzed by sonication with 1 mM phenylmethylsulfonyl fluoride added. After centrifugation of the sample, the supernatant was loaded onto a Ni-NTA column (Qiagen) equilibrated with buffer B (50 mM sodium phosphate pH 8.0; 500 mM NaCl; 20 mM imidazol; 10 mM β-mercaptoethanol) and eluted via an imidazol gradient. The NS5BΔ21 containing fractions were pooled and dialyzed against buffer C (50 mM Tris/HCl pH 7.6, 150 mM NaCl, 10% glycerol, and 10 mM dithiotreitol). A further purification step included a poly(U) column (Amersham Biosciences). Elution of the protein was performed with a NaCl gradient and yielded 99% pure protein. The NS5BΔ21-containing fractions were pooled and dialyzed against buffer D (50 mM Tris/HCl pH 7.6, 300 mM NaCl, 10% glycerol and 10 mM dithiotreitol). Enzyme concentration was routinely determined using an extinction coefficient at 280 nm of 80650 M^{-1} cm^{-1} in buffer E (6 M guanidinium hydrochloride and 20 mM sodium phosphate pH 6.5).

Buffers. All experiments were carried out at 25 °C, unless indicated otherwise, in buffer F containing 50 mM HEPES pH 7.5, 4 mM $MgCl_2$, 1 mM $MnCl_2$, 0.5% Triton X-100, and 10 mM dithiotreitol. Annealing buffer consisted of 25 mM cacodylate buffer pH 6.5, 25 mM NaCl, and 5 mM $MgCl_2$. Optimized conditions for primer-dependent synthesis were 50 mM HEPES, pH 7.5, 2 mM $MgCl_2$, 0.2 mM $MnCl_2$, 0.5% Triton X-100, and 10 mM dithiotreitol.

Nucleotides and Oligonucleotides. NTPs were purchased from Roche (Mannheim, Germany) and dinucleotides (GpU und GpC) were from Sigma. [α-^{32}P]-UTP (10 μCi/μL, 3000 Ci/mmol) was purchased from Amersham Biosciences (Freiburg, Germany).

Oligonucleotides were purchased from IBA (Göttingen, Germany) and purified using denaturing PAGE (15% acrylamide, 7 M urea) followed by elution from the gel using the Schleicher & Schuell Biotrap unit. The sequence of the 13/16-mer RNA/RNA p/t used for the binding studies was 5′-GCAGCGAGCAUCU and 5′-CUAAGAUGCUCGCUGC, respectively. The 5′-end of the 16-mer template was labeled with a FAM fluorophor. The sequence of the 19-mer RNA was 5′-UGUUAUAAUUAUUGUAUAC.

Primer oligonucleotides for the nucleotide incorporation studies were 5′-end-labeled with T4 polynucleotide kinase as described (*37*). Primer and template oligonucleotides were annealed by heating equimolar amounts in annealing buffer at 90 °C, followed by cooling to room temperature over several hours in a heating block. The completeness of the reaction was checked by native PAGE.

Fluorescence Titrations. Fluorescence titrations were performed using an SLM Smart 8100 spectrofluorimeter equipped with a PH-PC 9635 photomultiplier. Fluorescence of FAM was excited at 492 nm, and the emission was monitored at 516 nm (slit widths 1 and 16 nm, respectively). Data were evaluated using the program Grafit (Erithacus Software). The relative fluorescence was plotted against the corresponding protein concentration, and the dissociation constant was calculated using a quadratic equation. All experiments were carried out at 25 °C.

To determine the binding affinity via competition experiments, a preformed complex of labeled 16-mer RNA (40 nM) and NS5BΔ21 (141 nM) was titrated with unlabeled RNAs. The competitive titrations were evaluated by using the program Scientist (MicroMath Scientific Software), which allows the user to define the system under investigation as a series of parallel equations defining (in this case) each discrete equilibrium, the relationship between the total and free concentrations of the components, and the way in which the observable signal is generated.

Rapid Kinetics of RNA−NS5BΔ21 Interaction. Analysis of concentration dependent RNA-NS5BΔ21 association was performed using a Hi-Tech SF-61 MX Multi-Mixing stopped-flow spectrofluorimeter. The temperature in the sample-handling unit was maintained at 25 °C. 40 nM FAM 16-mer RNA was rapidly mixed with varying concentrations of NS5BΔ21 (150−400 nM), and the time courses of the fluorescence change were observed via a cutoff filter (530 nm) after excitation of the FAM fluorophor at 492 nm. Data were averaged over 10 experiments and analyzed using a single-exponential equation. All concentrations reported are final concentrations after mixing in the stopped-flow cell. Data were evaluated using the program Grafit (Erithacus Software).

The dissociation kinetic was analyzed under conditions described above. A preformed complex of 40 nM FAM 16-mer RNA (see above) and 200 nM NS5BΔ21 was rapidly mixed with 20 μM of poly(C)-RNA. Data analysis was performed as described above.

Oligomerization Studies. Oligomerization of NS5BΔ21 was analyzed using a dynamic light scattering device (DynaPro MS/X, Protein Solutions, UK). This device is capable of analyzing a size range of particles from 1 nm to 1 μm. All buffers and protein solutions were either carefully filtered or centrifuged and degassed to prevent scattering from suspended particles and bubbles. All measurements were performed at 20 °C.

Single Nucleotide Incorporation Studies. For single-turnover, single-nucleotide incorporation experiments, a preformed complex of p/t-NS5BΔ21 (208 nM dinucleotide-primer, 940 nM template, and 1.5 μM NS5BΔ21) was rapidly mixed with an excess of rNTP (250 μM) and stopped after various times. Data were fitted to a single-exponential burst equation. The effective transient nucleotide incorporation rate (k_{pol}) is derived from the exponential fit.

The affinity of ATP was determined by the dependence of the transient rate on the ATP concentration. To measure the affinity of the ATP to a preformed p/t-NS5BΔ21 complex (208 nM GpU-primer, 940 nM 19mer template, and 1.5 μM NS5BΔ21), the complex was rapidly mixed with various concentrations of ATP and quenched after $t_{1/2}$ of the maximal transient rate. The corresponding rates were then calculated from the concentration of elongated primer by converting the exponential equation into $k = -\ln[1 - ([P_{+1}]_t/[P]_0)]/t(\mathrm{s})$. $[P]_0$ corresponds to the concentration of the NS5BΔ21-p/t complex available for incorporation at $t = 0$, and t equals the reaction time ($t_{1/2}$ of the maximal transient rate). The rates observed were plotted against the ATP concentration, and the dissociation constant (K_d) was calculated by fitting the data to a hyperbola.

Products were analyzed by denaturing PAGE (22% polyacrylamide/7 M urea) and quantified by scanning the dried gel using a phosphorimager (Fuji FLA 5000). Data were evaluated using the program Grafit.

RESULTS

Interaction of NS5BΔ21 with a RNA/RNA p/t under Steady-State Conditions. Equilibrium titrations using a FAM fluorophor as probe attached to the 5′-end of the template were performed, to determine the affinity of NS5BΔ21 to a 13/16-mer RNA/RNA p/t. Figure 1 shows a titration curve

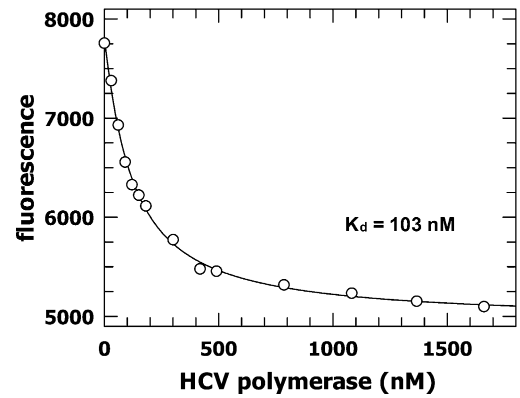

FIGURE 1: Fluorescence titration of partially double-stranded RNA with NS5BΔ21. A 13/16-mer p/t (40 nM) was titrated with NS5BΔ21 while monitoring the FAM fluorescence of the labeled template (excited at 492 nm and observed at 516 nm). The curve shows the best fit of the data to a quadratic equation yielding a dissociation constant (K_d) of 103 nM (± 7).

of a given p/t concentration (40 nM) with increasing amounts of NS5BΔ21 resulting in a decrease of the fluorescence signal of about 35%. By fitting the experimental data to a quadratic equation, an equilibrium constant (K_d) of 103 nM (± 7) for the p/t binding was determined. Fluorescence titrations in the presence of GTP (1 mM) known to increase the enzyme activity considerably (*28*) did not show any differences compared to titrations performed in the absence of GTP (data not shown).

Interaction of NS5BΔ21 with Single-Stranded RNA under Steady-State Conditions. Binding experiments with solely single-stranded RNA were performed, to determine if the weak binding affinity of the RNA/RNA p/t substrate described above, arises from the double strand. A titration of a FAM-labeled 16-mer RNA with NS5BΔ21 is shown in Figure 2a. The analysis of the experimental data yielded a K_d of 99 nM (± 15). Interestingly, the K_d determined for single-stranded RNA is in unpredictably good agreement with the K_d obtained with the partially double-stranded RNA substrate. Competition experiments with unlabeled RNA were performed to exclude that the observed signal might be affected by unspecific interactions between the fluorescence label and the protein. Accordingly, a preformed complex of 40 nM FAM-labeled 16-mer RNA and 141 nM NS5BΔ21 was titrated with unlabeled 16-mer RNA (Figure 2b) or unlabeled 13/16-mer RNA/RNA (data not shown). Data were fitted to a multi-equilibrium model, yielding binding affinities of 245 nM (± 21) and 251 nM (± 41), respectively. Additionally, we performed filter-binding experiments using radiolabeled RNAs. Again K_d's in the range of 250 nM were obtained (data not shown). These indirectly derived dissociation constants of unlabeled RNAs are approximately 2.5-fold higher than the K_d's determined for the labeled substrate, indicating the FAM label might have some effect on binding. Analogous experiments in the presence of high GTP concentrations (up to 1 mM) did not show any significant effect on the binding parameters (data not shown).

Detailed Characterization of RNA Binding under Pre-Steady-State Conditions. Stopped-flow experiments were performed to characterize the RNA−protein interaction in more detail. First, we examined if the RNA−NS5BΔ21 association occurs in a concentration-dependent manner. To address this question, equal volumes of RNA solution (40

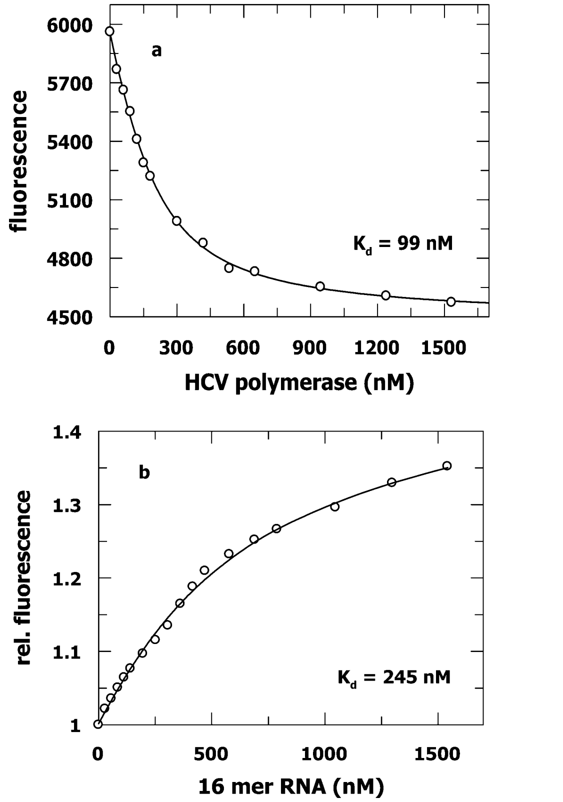

FIGURE 2: Fluorescence titrations of single-stranded RNA with NS5BΔ21. (a) 40 nM of a FAM-labeled 16-mer RNA was titrated with NS5BΔ21. The curve shows the best fit of the experimental data to a quadratic equation and gave a K_d of 99 nM (± 15). (b) Competition titration of labeled RNA with unlabeled RNA. A preformed 16-mer RNA−NS5BΔ21 complex (40 and 141 nM, respectively) was titrated with unlabeled 16-mer RNA. The displacement was monitored by observing the recovery of the fluorescence signal (excitation at 492 nm and emission at 516 nm) of the free FAM-labeled 16-mer RNA. The curve shows the best fit by least-squares fitting to a model describing the two binding equilibria from which a dissociation constant (K_d) of 245 nM (± 21) was obtained (see Materials and Methods).

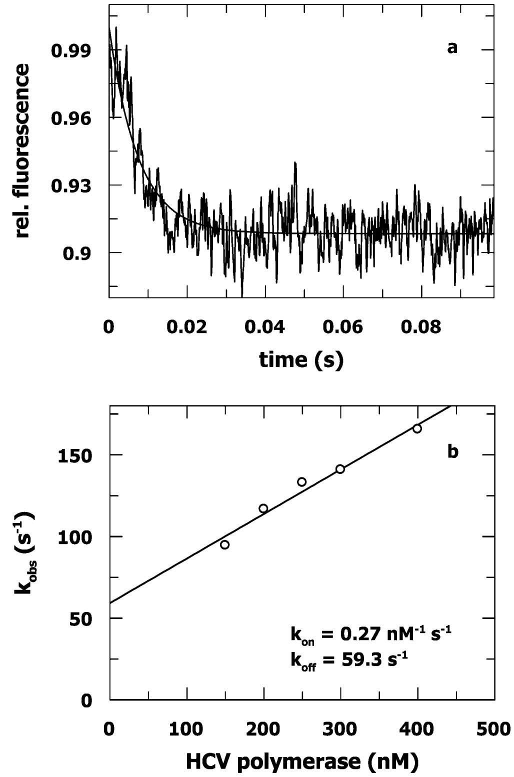

FIGURE 3: Transient kinetic analysis of the association of NS5BΔ21 and a 16-mer RNA. (a) Representative time course of the association kinetic of 250 nM NS5BΔ21 and 40 nM FAM-labeled 16-mer RNA. The curve shows the best fit to a single-exponential equation, yielding a pseudo-first-order rate constant (k_{obs}) of 133 s^{-1} (± 5.5). (b) Dependence of the fitted k_{obs} on the polymerase concentration. Data were analyzed via linear regression, yielding an association rate constant (k_{on}) of 0.27 nM^{-1} s^{-1} (± 0.027) and a dissociation rate constant of 59.3 s^{-1} (± 7.2).

nM) and NS5BΔ21 solution (150 to 400 nM) were rapidly mixed, and the time course of the fluorescence change was monitored. A representative time course of the association kinetic of a FAM-labeled 16-mer RNA (40 nM) with NS5BΔ21 (250 nM) is shown in Figure 3a. The data were fitted to a single-exponential equation yielding a pseudo-first-order rate constant (k_{obs}) of 133 s^{-1} (± 5.5). The secondary plot of the dependence of k_{obs} on the NS5BΔ21 concentration shows that the observed rates are concentration dependent. The data were fitted to a linear regression yielding a slope of 0.27 nM^{-1} s^{-1} (± 0.027), which corresponds to the association rate constant (k_{on}). The dissociation rate constant (k_{off}) derived from the intercept with the *y*-axis was 59 s^{-1} (± 7.2). This k_{off} could be confirmed by direct measurement of the dissociation reaction performing competition experiments with a preformed FAM 16-mer RNA-NS5BΔ21 complex and an excess of unlabeled polyC-RNA (k_{off}: 64,7 s^{-1}, data not shown). Dividing the observed dissociation rate constant (k_{off}) by the association rate constant (k_{on}), an overall affinity of 217 nM can be calculated. This calculated K_d value is in excellent agreement with the K_d value derived from the equilibrium titrations (see above).

Oligomerization. Several groups have proposed that oligomerization of HC-BK NS5B is an essential requirement for the polymerization reaction (*34*−*36*). To investigate this phenomenon, detailed analyses of HC-J4 NS5BΔ21 oligomerization using a dynamic light scattering (DLS) device were performed. First, we determined the degree of NS5BΔ21 oligomerization in the enzyme storage buffer (buffer D consisting of 50 mM Tris/HCl pH 7.6, 300 mM NaCl, 10% glycerol, and 10 mM dithiotreitol). Here, the polymerase showed no aggregation and was monomeric. Incubation of the samples for several days at 20 °C did not show any change, indicating that the protein is a stable monomer under these conditions. In a subsequent experiment, we analyzed the aggregation state of HC-J4 NS5BΔ21 diluted in assay buffer (buffer F without Triton X-100 consisting of 50 mM HEPES pH 7.5, 4 mM $MgCl_2$, 1 mM $MnCl_2$, and 10 mM dithiotreitol). Surprisingly, there was a drastic shift of the observable DLS signal (change of the hydrodynamic radius from 3.8 to 239 nm) representing the formation of high molecular weight oligomers. As the size range of particles the dynamic light scattering apparatus is able to analyze is 1 nm to 1 μm, we are well in the working range of the device. A careful analysis of buffer components revealed that NaCl is responsible for this shift. Figure 4 shows a plot of the ratio of monomeric NS5BΔ21 against the NaCl concentration (△). At salt concentrations below 150 mM NaCl HC-J4 polymerase (Δ21) is in a highly oligomeric, aggregated state. Concentrations above 150 mM caused a disruption of the oligomers leading to the formation of monomers. At 280 mM all protein is in the monomeric state. A more careful

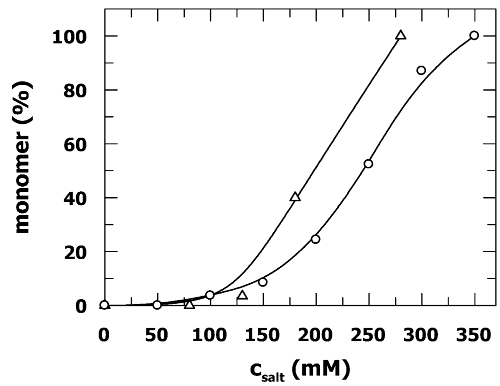

FIGURE 4: Correlation of NS5BΔ21 oligomerization on the monovalent salt concentration. The proportion of monomeric enzyme (7.2 μM) was determined at different NaCl (△) or KCl (○) concentrations using a DLS device.

analysis of this phenomenon clearly showed that the change in the oligomeric state is a fully reversible, salt-dependent process, whereas the establishment of the equilibrium is quite slow with about 60 min (95% completion, data not shown). Very similar data were obtained in KCl except for a slight increase in the monovalent salt concentration required to shift the equilibrium toward the monomeric state (Figure 4, ○). To exclude that the oligomerization that is measured with the DLS device is due to precipitation of the enzyme or solubility differences in different salt environments, we performed an additional experiment. For that matter, NS5BΔ21 was diluted in assay buffer (low salt) and incubated for 1 h to allow for oligomerization, followed by a centrifugation step for 30 min at 13 000 rpm. The polymerization reaction was then started by adding substrate. We did not observe any difference in polymerase activity between centrifuged samples and samples that had not been centrifuged nor did we find any polymerase activity in an imaginary "pellet" (data not shown).

Next we determined the influence of single-stranded RNA on the oligomerization state. First, RNA was added to monomeric HCV polymerase under high salt conditions (300 mM NaCl). Under those conditions, the RNA did not show any effect on the oligomeric state of NS5BΔ21. However, if the RNA was added to a solution containing oligomeric polymerase at low NaCl concentrations (50 mM), the recorded signal ran out of working range indicating further oligomerization of the sample. Additionally, we examined a possible influence of GTP on the oligomerization state of NS5BΔ21. It has been reported by Lohmann et al. (*28*) that high GTP concentrations lead to an increased activity of the HCV polymerase. Furthermore, according to a recent crystallographic study a second, GTP-specific low-affinity binding pocket has been proposed (*6*). This pocket appears to be located in a crystallographic lattice contact on the protein surface in close proximity to a proposed oligomerization interface (*36*). To examine if there is a correlation between the observed activity increase at high GTP concentrations possibly induced via binding to a second GTP-specific nucleotide pocket resulting in a shift of the aggregation equilibrium toward oligomers, comparative DLS measurements in the presence or absence of GTP at different NaCl concentrations were performed. However, under the conditions tested, there was no detectable difference with respect

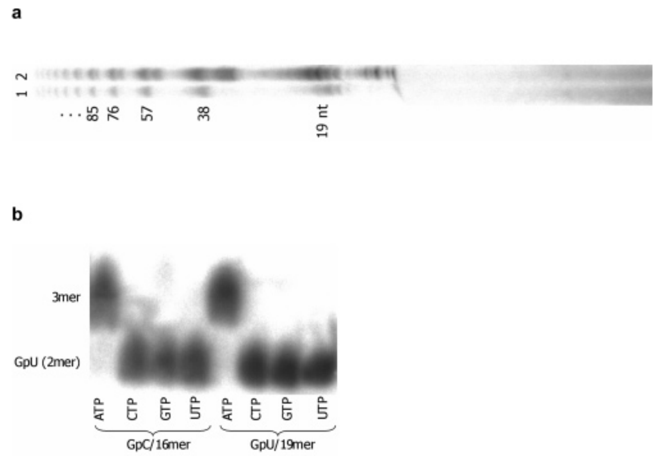

FIGURE 5: RNA synthesis by NS5BΔ21. (a) De novo synthesis − a preformed complex of 94 nM 19-mer RNA template and 360 nM NS5BΔ21 was mixed with all four rNTPs (500 μM GTP, 250 μM ATP, CTP, and UTP plus 100 nCi [α-^{32}P]-UTP). Reaction was stopped by adding formamide buffer after an incubation period of 2 h at 23 °C. Products were analyzed by denaturing PAGE (lane 1 + 2 differ in the concentration of cold UTP added; 250 μM versus 25 μM). (b) Dinucleotide primer-dependent synthesis − 1.5 μM HCV polymerase was incubated for 20 min at 20 °C with 940 nM RNA template (19- or 16-mer) and 208 nM of the corresponding, radioactively labeled dinucleotide primer. The enzymatic reaction was started by adding 250 μM ATP, CTP, GTP, or UTP and stopped after 60 min with formamide buffer. Products were analyzed by denaturing PAGE.

to the oligomerization behavior of NS5BΔ21 (data not shown).

Nucleotide Incorporation Studies. First, we examined primer-dependent nucleotide incorporation by NS5BΔ21. Using a homopolymeric substrate (polyA$_{300}$/oligoU$_{15}$), some elongation of the radioactive labeled 15-mer oligoU-primers was observed as already described by others (*17*, *18*, *20*). Interestingly, the products were longer than expected given the template length of ca. 300 nt's. The overall efficiency of nucleotide incorporation by HCV NS5BΔ21 was very low (data not shown). Next, we performed single-nucleotide incorporation studies with short, partially double-stranded RNA/RNA p/t to further characterize the underlying mechanism of primer-dependent RNA synthesis by the HCV polymerase. However, neither a 13/16-mer nor a 20/35 or a 20/100 p/t, which have been shown to bind to the HCV polymerase (see above), showed any detectable nucleotide incorporation.

Since these RNAs were not appropriate to study mechanistic aspects of the NS5B catalyzed nucleotide incorporation reaction, we turned our attention toward de novo synthesis in the absence of any primer. The following experiments were carried out with either a 19-mer RNA previously shown to act as substrate (*38*) or a 16-mer RNA. With both the 19-mer and the 16-mer template RNAs, synthesis in the presence of all four ribonucleotides yielded the expected products (19 or 16 nucleotides), albeit the overall efficacy of the reaction in the case of the 16-mer was significantly lower. Intriguingly, in addition to the expected products, there was a cluster of RNAs corresponding to multiple length of the input RNA template (Figure 5a, lanes 1 and 2). The 3′-hydroxyl group (*17*) of the 19-mer RNA template was oxidized to preclude the formation of longer RNAs, which possibly could have resulted from ligation events between newly synthesized RNA molecules and the template. Yet, no difference with respect to these longer products could be observed between oxidized or "regular" RNA template. Furthermore, incubation of in vitro synthesized RNA with HCV polymerase did not show any ligation products, indicating the observed multiple template-sized products were not generated by bacterial ligase impurities contained in the HCV polymerase preparation. Interestingly, in the presence of GMP as initiation nucleotide, the de novo synthesis did not show these high molecular weight species. To test if this experimental setup can be used to study single nucleotide incorporation, polymerase and RNA template were incubated with the initiation GTP, and then the next nucleotide to be incorporated according to the template sequence was added. Over a period of 2 h, formation of a newly synthesized dinucleotide could not be observed.

Accordingly, a further approach to analyze the NS5B nucleotide incorporation reaction in more detail was tested. Instead of oligomeric RNA primers (see above), we now used dinucleotides in combination with the aforementioned 19-mer and 16-mer template RNAs to initiate the reaction. 1.5 μM HCV polymerase was incubated for 20 min at 20 °C with 940 nM RNA template (19-mer or 16-mer) and 208 nM of the corresponding, radioactively labeled dinucleotide (GpU or GpC). The enzymatic reaction was started by adding 250 μM ATP, CTP, GTP, or UTP and stopped after 60 min with formamide buffer. Only in the case of the correct incoming nucleotide (ATP in this case) primer extension was observed (Figure 5b). Next, we analyzed the time course of single-turnover, single-nucleotide incorporation into the 2/19 RNA/RNA p/t. Incorporation of ATP occurred in a monophasic kinetic resulting in the complete elongation of the dinucleotide primer (Figure 6a). Fitting the experimental data to a single-exponential equation yielded an incorporation rate (k_{pol}) of 0.0007 s^{-1} ($\pm$ 0.00003). To ensure that the observed single-turnover rate of incorporation was not limited by binding parameters, we carefully examined the binding affinities of the incoming ATP. The affinity was determined by plotting the observed rates at various concentrations of ATP and fitting the data to a hyperbola resulting in a dissociation constant (K_d) of 27.7 μM ($\pm$ 1.2) (Figure 6b). Interestingly, compared to elongation (data not shown), the initiation is highly specific for the canonical base pair as absolutely no misincorporation was observed (Figure 5b).

As described above, several RNA templates used in this study could not be utilized by the NS5BΔ21 as substrate in nucleotide incorporation assays, although binding studies indicated reasonable protein−RNA interaction. A possible explanation for this finding could be RNA bound in an orientation not properly positioned for initiation of RNA synthesis. Accordingly, there might be several binding modes showing different affinities. Aiming to resolve this issue, we measured the rate of nucleotide incorporation on the template concentration (Figure 7). Fitting of the experimental data to a hyperbolic equation yielded a K_d of 260 nM ($\pm$ 22) for the 2/19 RNA/RNA p/t. This value is in excellent agreement with values obtained via equilibrium titrations (see above).

Finally, we tested whether there is a correlation between NS5BΔ21 oligomerization and polymerase activity as proposed by others (*34*−*36*). As outlined above, there is a salt-dependent equilibrium between the monomeric and the oligomeric state of the protein (Figure 4). Upon dilution of

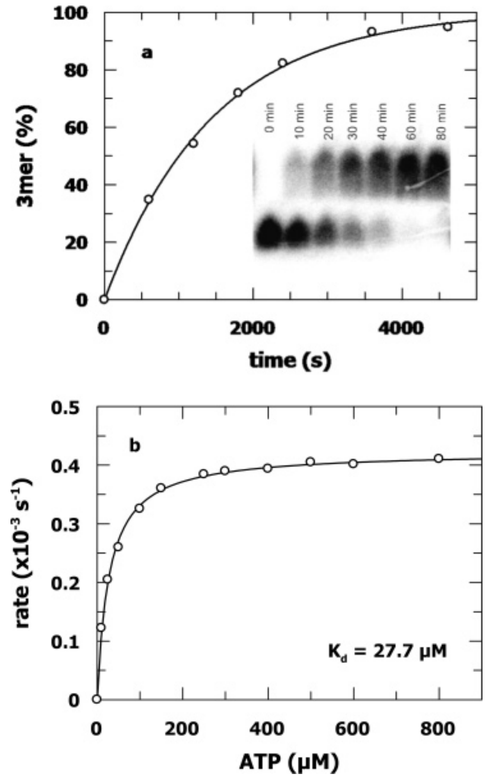

FIGURE 6: Single-turnover, single-nucleotide incorporation into a 2/19 RNA/RNA p/t by NS5BΔ21. (a) A preformed complex of 208 nM GpU-primer, 940 nM 19-mer template and 1.5 μM NS5BΔ21 was rapidly mixed with 250 μM ATP. Reactions were stopped at time points given. The curve shows the best fit of the data to a single-exponential equation yielding a k_{pol} of 0.0007 s^{-1} ($\pm$ 0.00003). The inset shows the PAGE analysis of the reaction. (b) Analysis of the binding affinity of the incoming nucleotide. Increasing amounts of ATP were rapidly mixed with a preformed complex of 208 nM GpU-primer, 940 nM 19-mer template and 1.5 μM NS5BΔ21 and quenched after $\tau_{1/2}$ of the maximal transient rate (see Figure 6a). Data were fitted to a hyperbolic equation, yielding a K_d value of 27.7 μM ($\pm$ 1.2).

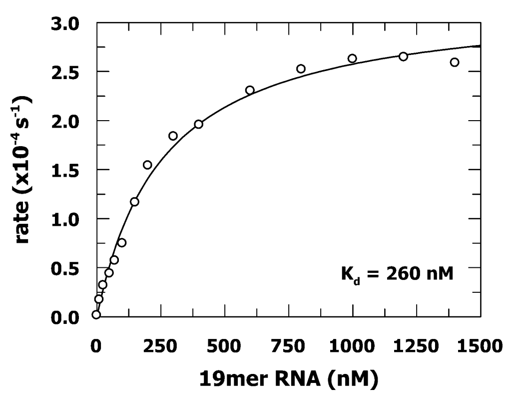

FIGURE 7: Dependence of the transient nucleotide incorporation rate on the 19-mer RNA substrate concentration. Increasing amounts of 19-mer template were rapidly mixed with a preformed complex of 208 nM GpU-primer, 1.5 μM NS5BΔ21 and 250 μM ATP. The reaction was stopped after $\tau_{1/2}$ of the maximal transient rate (see Figure 6a). Data were fitted to a hyperbola resulting in a K_d value of 260 nM ($\pm$ 22).

monomeric NS5BΔ21 from high salt into a low salt buffer, oligomerization is initiated, and the new equilibrium is reached after about 60 min. At certain time points after mixing monomeric HCV polymerase with RNA template and dinucleotide primer in low salt reaction buffer, the enzymatic reaction was started by adding 250 μM ATP and stopped

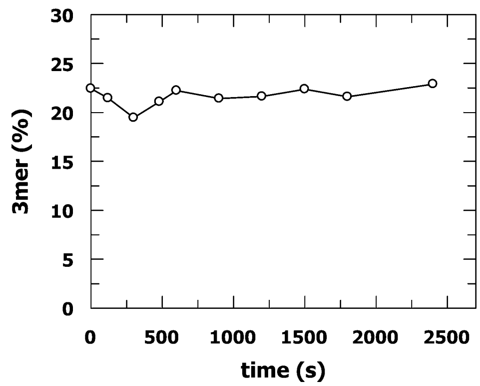

FIGURE 8: Dependence of the transient nucleotide incorporation rate on the oligomeric state of NS5BΔ21. At certain time points after mixing monomeric HCV polymerase with RNA template and dinucleotide-primer in low salt reaction buffer (see Materials and Methods) inducing oligomerization of the protein, the enzymatic reaction was started by adding 250 μM ATP and stopped after $\tau_{1/2}$ of the maximal transient rate (see Figure 6a). Here the different time points represent different aggregation states of NS5BΔ21, whereas t_0 = 100% monomer, t_{2500} > 90% oligomers, and time points between = mixture of monomers, dimers, and oligomers (as determined by DLS).

after $\tau_{1/2}$ of the maximal transient rate (Figure 8). In contrast to data published previously, we could not observe any significant increase in polymerase activity upon oligomerization of NS5BΔ21.

DISCUSSION

The RNA-dependent RNA polymerase of HCV is a major target for the development of antiviral drugs against this potentially deadly viral disease. However, our current understanding of this enzyme is rather rudimentary, and many reports about this polymerase are, at least in part, inconsistent. The reasons for this predicament are manifold. Missing protein cofactors or replicase components, poor enzymatic activity of the core polymerase, membrane association, solubility problems, and biochemical differences between enzymes derived from different isolates are but a few of the aspects that may have hampered unraveling mechanistic details of the enzymatic reaction catalyzed by NS5B. As a result, so far no adequate in vitro assays are available for this enzyme hindering drug development. In the present study we have tried to untangle some of the intrinsic problems accompanied with this protein by applying quantitative biochemical and kinetic analyses. We managed to derive quantitative data which might help to define the mechanistic properties of NS5B catalyzed HCV replication.

In this study, we provide direct experimental evidence for the first time to show that NS5BΔ21 binds to partially double-stranded RNA/RNA p/t. Using a FAM-labeled 13/16mer p/t and performing fluorescence measurements, we derived a dissociation constant (K_d) of 103 nM, equivalent to the K_d determined for the binding of single-stranded RNA to NS5BΔ21. To confirm this result, fluorescence competition titrations with unlabeled RNAs (single as well as partially double stranded) were carried out, revealing a K_d of ca. 250 nM. Thus, the fluorophor seems to have only minor effects on binding and, with an approximately 2.5-fold discrepancy, the dissociation constants are in fairly good agreement. Yet, we cannot entirely rule out the probability that the 13/16-mer is bound via the three single-stranded nucleotides of the template. On the other hand, it has been shown that the minimal template length is 5 nt (*13*). Analyzing RNA binding via nucleotide incorporation (Figure 7) confirmed a K_d of about 260 nM for the interaction with the 19-mer RNA substrate, apparently indicating the complex observed in the fluorescence binding studies represents a catalytically competent protein−substrate complex.

Taken together, the K_d values determined in this study, using different RNA substrates and applying several complementary techniques, indicate that the HCV polymerase binds such RNAs with a rather low affinity compared to other polymerases. Molecular modeling of potential RNA substrates into the NS5B structure (*3*−*5*) and a crystal structure of a binary NS5BΔ21−RNA complex (*8*) suggest numerous polar contacts and van der Waals interactions between the enzyme and the nucleic acid substrate. The protein/RNA interactions in the crystal structure have been found to be nonspecific, and the electron density corresponding to the 5-mer ssRNA indicates that the template appears to be sliding back and forth in the binding cleft on the NS5B fingers domain (*8*). The surprisingly high K_d measured is consistent with the crystallographic data and is in good agreement with the low RNA substrate specificity of NS5B reported previously (*13*, *17*, *18*, *21*, *22*, *26*−*28*) and with the K_d values published for the binding of the polymerase to NS5B-X-RNA (*39*, *40*). This also lends support to the notion that the HCV polymerase either needs additional viral or host-encoded factors to increase substrate specificity, and/or it binds an, as yet unidentified, specific sequence of the HCV genome. A potential binding site for such a factor could be the arm-like motif in the thumb domain (*4*), which in other, nonrelated proteins is responsible for the interaction with proteins or peptides. Alternatively, it has been suggested that GTP could increase the RNA binding affinity by inducing a conformational rearrangement or oligomerization of the protein. However, our biochemical and kinetic data do not support such a scenario.

Upon investigating the association kinetics of NS5BΔ21 with the 16-mer RNA oligomer using the stopped-flow technique, we observed a nearly diffusion controlled, one-step binding reaction with a second-order association rate constant (k_{on}) of 0.273 nM^{-1} s^{-1}. The intercept of the plot of the dependence of the pseudo-first-order rate constant of RNA binding on the NS5B concentration yielded a dissociation rate constant (k_{off}) of 59.3 s^{-1} in excellent agreement with transient fluorescence competition measurements (k_{off}: 64.7 s^{-1}, data not shown). Using these numbers, we calculated an overall affinity of 217 nM for the NS5BΔ21−16-mer RNA interaction. Again, this value is in excellent agreement with the fluorescence titrations confirming the quality of the data presented. The transient binding measurements corroborate the data obtained from X-ray cocrystal structures. Here, extensive interactions between the fingers and the thumb domains have been observed keeping the polymerase in a rigid, closed conformation even in the absence of an RNA substrate (*3*−*5*, *8*). A similar overall structure has been shown for the bovine viral diarrhea virus (BVDV) NS5B (*9*), bacteriophage ϕ6 polymerase (*10*), reovirus lambda3 protein (*11*), and foot-and-mouth disease virus 3D polymerase (*12*). Thus, initial substrate binding is likely to take place without extensive conformational changes of the enzyme.

Oligomerization of the HCV polymerase has been suggested to be crucial for the activity of this enzyme (*34*−*36*). In the present study, we have performed extensive DLS measurements in the presence and in the absence of substrates to analyze NS5B protein−protein interactions and potential implications for RNA synthesis. We are able to show that oligomerization of NS5BΔ21 is a dynamic, NaCl- or KCl-dependent process, while low salt conditions leads to aggregates and in high salt conditions (> 280 mM) the protein exists as a stable monomer, indicating that the majority of the interface contacts are of an ionic nature. This finding is in agreement with Wang et al. (*36*) but inconsistent to some extent with other studies (*35*, *41*) in which the enzyme was shown to be monomeric or dimeric at lower NaCl concentrations (150−200 mM). These differences could be due to the fact, that these RdRps are derived from the HC-BK isolate as compared to HC-J4 used in this study. There are 24 differences between the primary structures of the J4 and the BK isolates, and these are clustered in four regions and are located on the protein surface (*8*). DLS measurements in the presence of RNA at low NaCl concentrations show that highly oligomeric NS5BΔ21 is capable of binding RNA. The observation that the DLS signal for such complexes runs out of range evidently indicates further oligomerization triggered by the nucleic acid in agreement with data obtained by Labonté et al. (*41*). To what extent monomeric HCV polymerase is capable of binding nucleic acids cannot be answered as the high salt concentration necessary to stabilize the monomeric state strongly interferes with RNA binding (data not shown). Performing nucleotide incorporation studies with NS5BΔ21 in different aggregation states did not show any correlation between catalytic activity and oligomerization in contradiction to other reports (*34*−*36*). The reason for this discrepancy remains unclear.

HCV polymerase has been shown to be capable of initiating RNA replication via a primer-dependent, a copy back, and/or a de novo synthesis mechanism. In our hands, using short RNA/RNA p/t a primer-dependent synthesis could not be detected, although these RNAs were shown to bind NS5BΔ21. It can be speculated that these nucleic acids are either bound in a catalytically incompetent conformation or that the initiation is blocked for some other reason. In our hands, primer elongation could only be observed with long homopolymeric template substrates as has been shown previously (*17*, *18*, *20*, *26*).

Analyzing de novo and dinucleotide-dependent synthesis using a 19-mer RNA template, the expected product, as well as RNA species corresponding to a multiple length of the template, has been identified. These unexpected products are often up to six times longer than the template RNA. We showed that ligation events due to impurities or an intrinsic ligase activity of the polymerase can be excluded. As suggested for several viral RNA polymerases (*42*−*48*) including NS5B (*23*, *25*, *38*), these products are most likely the result of template switching events. So-called "end-to-end" and/or "internal template switching" mechanisms have been described. In this study, we could not observe any template switching products with NS5BΔ21 when initiating RNA synthesis with GMP. This finding strongly suggests an "end-to-end" template switching mode (Figure 9). Additionally, the absence of template switching events in the presence of a nucleic acid competitor trapping the polymerase

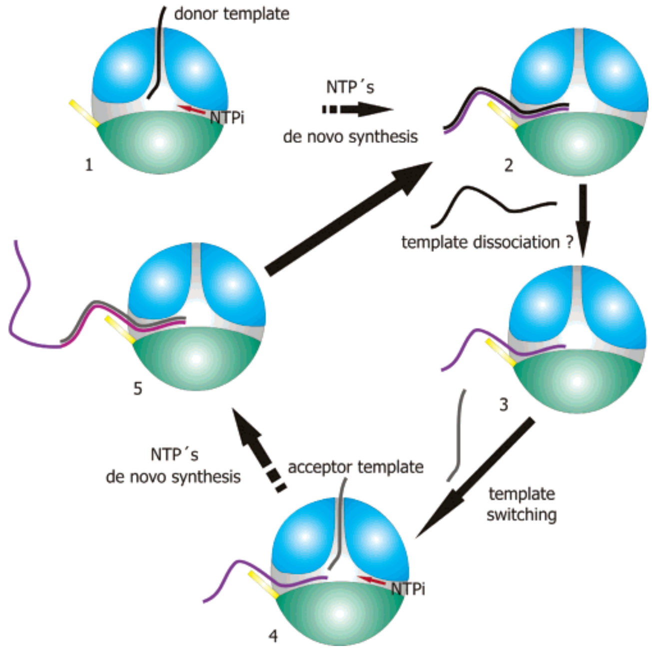

FIGURE 9: Model of the proposed template switching mechanism by HCV NS5B. The fingers (blue), thumb (green), and palm (grey) domains are shown schematically. The β-hairpin is shown in yellow. (1) Formation of the initiation complex consisting of NS5B, template, and incoming nucleotide. (2) De novo synthesis of the complementary strand. (3) Dissociation of the template with the newly synthesized RNA staying bound to the enzyme. (4) Template switching event via binding of an acceptor template and the incoming nucleotide. (5) De novo synthesis of the complementary RNA strand to the 3′-end of the newly synthesize RNA. Now additional template switching events may take place (2−5) resulting in a RNA product of multiple template length.

(data not shown) indicates that the enzyme does not perform continuous RNA synthesis from the nascent RNA without dissociating from the template as described for poliovirus (*47*) and bovine viral diarrhea virus (BVDV) RNA polymerase (*46*). Furthermore, it appears that no stabilization is required by base pairing of the newly synthesized RNA with the next incoming RNA template for template switching events to occur. Thus, a "base-pairing-independent" template switching model (*48*) would explain why the products of the HCV NS5B reaction are exact multiples of the RNA template.

Analyzing single-turnover, single-nucleotide incorporation using a dinucleotide as a primer and a 16- or 19-mer as a template, an incorporation rate (k_{pol}) of 0.0007 s^{-1} was observed. Over a period of about 60 min, all primers were extended by one nucleotide. To exclude that the observed incorporation reaction is due to a low-level steady-state turnover by a small percentage of active enzyme, we performed incorporation experiments in the presence of a trap (dinucleotide primer or single-stranded RNA). Here we still observed extension of about 40% of the dinucleotide primers (data not shown). This finding was rather surprising as the off-rate (dissociation of the polymerase from the RNA substrate; 59.3 s^{-1} see above) is orders of magnitude faster than the incorporation reaction and suggests the existence of a highly stable protein/RNA p/t complex (see below).

The slow incorporation rate observed in this study certainly does not reflect the true polymerization rate of this enzyme but rather the rate of initiation of RNA synthesis, which appears to be rate limiting. There are several reports showing that in vitro NS5B is able to copy the full-length viral RNA genome within 1−2 h, albeit with a very low efficacy (<3% of the input RNA template is turned over) (*17*, *18*, *27*, *49*, *50*). In other words, once the slow initiation step has occurred, NS5B may elongate more like a “normal” polymerase. However, this extremely slow initiation renders a quantitative analysis of the elongation process very difficult if not impossible, when applying standard procedures, since the rates determined represent a mixture of both processes. In this study, we therefore focused on the early steps of RdRp catalytic cycle using short synthetic RNA substrates.

The analysis of the affinity of the incoming nucleotide, as determined by incorporation studies, revealed a K_d of 27.7 μM. This value is in good agreement with many other studies on several polymerases; thus it seems very unlikely that nucleotide binding causes any restrictions during the initiation step. It is difficult to pinpoint the exact reason for the slow initiation step. However, it is conceivable that the polymerase domain has to undergo a slow rate-limiting conformational change after initial binding of the substrates (template and dinucleotide primer) prior to incorporation (e.g., opening up of the C-terminal domain enabling translocation of the initiation complex) (*10*).

To further address this question, we performed competition experiments of an NS5BΔ21-template-^{32}P-labeled-GpU-primer complex with a large excess of unlabeled primer. After incubation of this initiation complex with the trap for certain time intervals, the polymerase reaction was started by adding nucleotide substrate. Under those conditions, we still observed about 25−40% extended primers, even after preincubation with the competitor for up to 40 min, indicating a highly stable complex (Cramer, J., to be published elsewhere). Despite that, the observed incorporation kinetics of these stable complexes was not any faster. Accordingly, there are two different polymerase/nucleic acid complexes: a very stable one (representing about 30% of the complexes) and a complex with a fast off-rate (representing about 70% of the complexes). Taken together, these data suggest that a conformational change does indeed occur. However, whether this structural rearrangement is a prerequisite for initiation or whether it can be accelerated by a specific viral RNA sequence or additional protein components, we currently can only speculate.

In conclusion, our studies show that in vitro HCV NS5BΔ21 is characterized by a distinct lack of efficiency. The K_d determined for RNA binding and the rates for single-nucleotide incorporation are orders of magnitude lower than one would expect for a replicative polymerase. Thus, it seems obvious that important cofactors are missing. This holds especially true for the initiation of RNA synthesis as reflected by the exceptionally low incorporation rates. On the other hand, with viral or host cofactors remaining unidentified, the dinucleotide-dependent HCV RdRp assay presented here permits the first quantitative analysis of nucleotide incorporation events and could serve as a kinetically well-defined model and as a valuable tool to develop and characterize potential NS5B inhibitors.

ACKNOWLEDGMENT

We thank Damien O’Farrell and Rachel Trowbridge for their help and advice during initial stages of the project, Jens Bukh and the NIAID/NIH for providing the clone pCV-J4L6S, and Roger S. Goody for continuous support.

REFERENCES

1. WHO (1999) Global surveillance and control of hepatitis C, *J. Viral Hepat. 6*, 35−47.
2. Heathcote, J., and Main, J. (2005) Treatment of hepatitis C, *J. Viral Hepat. 12*, 223−235.
3. Ago, H., Adachi, T., Yoshida, A., Yamamoto, M., Habuka, N., Yatsunami, K., and Miyano, M. (1999) Crystal structure of the RNA-dependent RNA polymerase of hepatitis C virus, *Structure 7*, 1417−1426.
4. Bressanelli, S., Tomei, L., Roussel, A., Incitti, I., Vitale, R. L., Mathieu, M., De Francesco, R., and Rey, F. A. (1999) Crystal structure of the RNA-dependent RNA polymerase of hepatitis C virus, *Proc. Natl. Acad. Sci. U.S.A. 96*, 13034−13039.
5. Lesburg, C. A., Cable, M. B., Ferrari, E., Hong, Z., Mannarino, A. F., and Weber, P. C. (1999) Crystal structure of the RNA-dependent RNA polymerase from hepatitis C virus reveals a fully encircled active site, *Nat. Struct. Biol. 6*, 937−943.
6. Bressanelli, S., Tomei, L., Rey, F. A., and De Francesco, R. (2002) Structural analysis of the hepatitis C virus RNA polymerase in complex with Ribonucleotides, *J. Virol. 76*, 3482−3492.
7. Yanagi, M., St Claire, M., Shapiro, M., Emerson, S. U., Purcell, R. H., and Bukh, J. (1998) Transcripts of a chimeric cDNA clone of hepatitis C virus genotype 1b are infectious in vivo, *Virology 244*, 161−172.
8. O’Farrell, D., Trowbridge, R., Rowlands, D., and Jäger, J. (2003) Substrate complexes of hepatitis C virus RNA polymerase (HC-J4): structural evidence for nucleotide import and de-novo initiation, *J. Mol. Biol. 326*, 1025−1035.
9. Choi, K. H., Groarke, J. M., Young, D. C., Kuhn, R. J., Smith, J. L., Pevear, D. C., and Rossmann, M. G. (2004) The structure of the RNA-dependent RNA polymerase from bovine viral diarrhea virus establishes the role of GTP in de novo initiation, *Proc. Natl. Acad. Sci. U.S.A. 101*, 4425−4430.
10. Butcher, S. J., Grimes, J. M., Makeyev, E. V., Bamford, D. H., and Stuart, D. L. (2001) A mechanism for initiating RNA-dependent RNA polymerization, *Nature 410*, 235−240.
11. Tao, Y., Farsetta, D. L., Nibert, M. L., and Harrison, S. C. (2002) RNA synthesis in a cage − structural studies of reovirus polymerase lambda3, *Cell 111*, 733−745.
12. Ferrer-Orta, C., Arias, A., Perez-Luque, R., Escarmis, C., Domingo, E., and Verdaguer, N. (2004) Structure of foot-and-mouth disease virus RNA-dependent RNA polymerase and its complex with a template-primer RNA, *J. Biol. Chem. 279*, 47212−47221.
13. Zhong, W., Ferrari, E., Lesburg, C. A., Maag, D., Ghosh, S. K., Cameron, C. E., Lau, J. Y., and Hong, Z. (2000) Template/primer requirements and single nucleotide incorporation by hepatitis C virus nonstructural protein 5B polymerase, *J. Virol. 74*, 9134−9143.
14. Hong, Z., Cameron, C. E., Walker, M. P., Castro, C., Yao, N. H., Lau, J. Y. N., and Zhong, W. D. (2001) A novel mechanism to ensure terminal initiation by hepatitis C virus NS5B polymerase, *Virology 285*, 6−11.
15. Adachi, T., Ago, H., Habuka, N., Okuda, K., Komatsu, M., Ikeda, S., and Yatsunami, K. (2002) The essential role of C-terminal residues in regulating the activity of hepatitis C virus RNA-dependent RNA polymerase, *Biochim. Biophys. Acta 1601*, 38−48.
16. Ranjith-Kumar, C. T., Gutshall, L., Sarisky, R. T., and Kao, C. C. (2003) Multiple interactions within the hepatitis C virus RNA polymerase repress primer-dependent RNA synthesis, *J. Mol. Biol. 330*, 675−685.
17. Behrens, S.-E., Tomei, L., and De Francesco, R. (1996) Identification and properties of the RNA-dependent RNA polymerase of hepatitis C virus, *EMBO J. 15*, 12−22.
18. Lohmann, V., Korner, F., Herian, U., and Bartenschlager, R. (1997) Biochemical properties of hepatitis C virus NS5B RNA-dependent RNA polymerase and identification of amino acid sequence motifs essential for enzymatic activity, *J. Virol. 71*, 8416−8428.
19. Luo, G. X., Hamatake, R. K., Mathis, D. M., Racela, J., Rigat, K. L., Lemm, J., and Colonno, R. J. (2000) De novo initiation of RNA synthesis by the RNA-dependent RNA polymerase (NS5B) of hepatitis C virus, *J. Virol. 74*, 851−863.
20. Johnson, R. B., Sun, X. L., Hockman, M. A., Villarreal, E. C., Wakulchik, M., and Wang, Q. M. (2000) Specificity and mech-

anism analysis of hepatitis C virus RNA-dependent RNA polymerase, *Arch. Biochem. Biophys. 377*, 129−134.

21. Oh, J. W., Ito, T., and Lai, M. M. C. (1999) A recombinant hepatitis C virus RNA-dependent RNA polymerase capable of copying the full-length viral RNA, *J. Virol. 73*, 7694−7702.
22. Hagedorn, C. H., van Beers, E. H., and De Staercke, C. (2000) Hepatitis C virus RNA-dependent RNA polymerase (NS5B polymerase), *Curr. Top. Microbiol. Immunol. 242*, 225−260.
23. Kao, C. C., Yang, X., Kline, A., Wang, Q. M., Barket, D., and Heinz, B. A. (2000) Template requirements for RNA synthesis by a recombinant hepatitis C virus RNA-dependent RNA polymerase, *J. Virol. 74*, 11121−11128.
24. Sun, X. L., Johnson, R. B., Hockman, M. A., and Wang, Q. M. (2000) De novo RNA synthesis catalyzed by HCV RNA-dependent RNA polymerase, *Biochem. Biophys. Res. Commun. 268*, 798−803.
25. Zhong, W. D., Uss, A. S., Ferrari, E., Lau, J. Y. N., and Hong, Z. (2000) De novo initiation of RNA synthesis by hepatitis C virus nonstructural protein 5B polymerase, *J. Virol. 74*, 2017−2022.
26. Lohmann, V., Roos, A., Korner, F., Koch, J. O., and Bartenschlager, R. (1998) Biochemical and kinetic analyses of NS5B RNA-dependent RNA polymerase of the hepatitis C virus, *Virology 249*, 108−118.
27. Yamashita, T., Kaneko, S., Shirota, Y., Qin, W., Nomura, T., Kobayashi, K., and Murakami, S. (1998) RNA-dependent RNA polymerase activity of the soluble recombinant hepatitis C virus NS5B protein truncated at the C-terminal region, *J. Biol. Chem. 273*, 15479−15486.
28. Lohmann, V., Overton, H., and Bartenschlager, R. (1999) Selective stimulation of hepatitis C virus and pestivirus NS5B RNA polymerase activity by GTP, *J. Biol. Chem. 274*, 10807−10815.
29. Restle, T., Müller, B., and Goody, R. S. (1990) Dimerization of Human-Immunodeficiency-Virus Type-1 Reverse-Transcriptase − A Target for Chemotherapeutic Intervention, *J. Biol. Chem. 265*, 8986−8988.
30. Kohlstaedt, L. A., Wang, J., Friedman, J. M., Rice, P. A., and Steitz, T. A. (1992) Crystal-Structure at 3.5 Angstrom Resolution of Hiv-1 Reverse-Transcriptase Complexed with An Inhibitor, *Science 256*, 1783−1790.
31. Pata, J. D., Schultz, S. C., and Kirkegaard, K. (1995) Functional oligomerization of poliovirus RNA-dependent RNA polymerase, *RNA 1*, 466−477.
32. Hansen, J. L., Long, A. M., and Schultz, S. C. (1997) Structure of the RNA-dependent RNA polymerase of poliovirus, *Structure 5*, 1109−1122.
33. Hobson, S. D., Rosenblum, E. S., Richards, O. C., Richmond, K., Kirkegaard, K., and Schultz, S. C. (2001) Oligomeric structures of poliovirus polymerase are important for function, *EMBO J. 20*, 1153−1163.
34. Qin, W., Yamashita, T., Shirota, Y., Lin, Y., Wei, W., and Murakami, S. (2001) Mutational analysis of the structure and functions of hepatitis C virus RNA-dependent RNA polymerase, *Hepatology 33*, 728−737.
35. Qin, W., Luo, H., Nomura, T., Hayashi, N., Yamashita, T., and Murakami, S. (2002) Oligomeric interaction of hepatitis C virus NS5B is critical for catalytic activity of RNA-dependent RNA polymerase, *J. Biol. Chem. 277*, 2132−2137.
36. Wang, Q. M., Hockman, M. A., Staschke, K., Johnson, R. B., Case, K. A., Lu, J., Parsons, S., Zhang, F., Rathnachalam, R., Kirkegaard, K., and Colacino, J. M. (2002) Oligomerization and cooperative RNA synthesis activity of hepatitis C virus RNA-dependent RNA polymerase, *J. Virol. 76*, 3865−3872.
37. Thrall, S. H., Krebs, R., Wöhrl, B. W., Cellai, L., Goody, R. S., and Restle, T. (1998) Pre-steady-state kinetic characterization of RNA-primed initiation of transcription by HIV-1 reverse transcriptase and analysis of the transition to a processive DNA-primed polymerization mode, *Biochemistry 37*, 13349−13358.
38. Ranjith-Kumar, C. T., Kim, Y. C., Gutshall, L., Silverman, C., Khandekar, S., Sarisky, R. T., and Kao, C. C. (2002) Mechanism of de novo initiation by the hepatitis C virus RNA-dependent RNA polymerase: Role of divalent metals, *J. Virol. 76*, 12513−12525.
39. Oh, J. W., Sheu, G. T., and Lai, M. M. C. (2000) Template requirement and initiation site selection by hepatitis C virus polymerase on a minimal viral RNA template, *J. Biol. Chem. 275*, 17710−17717.
40. Vo, N. V., Sheu, G. T., and Lai, M. M. C. (2003) Identification of RNA ligands that bind hepatitis C virus polymerase selectively and inhibits its RNA synthesis from the natural viral templates, *Virology 307*, 301−316.
41. Labonte, P., Axelrod, V., Agarwal, A., Aulabaugh, A., Amin, A., and Mak, P. (2002) Modulation of hepatitis C virus RNA-dependent RNA polymerase activity by structure-based site-directed mutagenesis, *J. Biol. Chem. 277*, 38838−38846.
42. Nudler, E., Avetissova, E., Markovtsov, V., and Goldfarb, A. (1996) Transcription processivity: Protein-DNA interactions holding together the elongation complex, *Science 273*, 211−217.
43. Tang, R. S., Barton, D. J., Flanegan, J. B., and Kirkegaard, K. (1997) Poliovirus RNA recombination in cell-free extracts, *RNA 3*, 624−633.
44. Murthy, V., Meijer, W. J. J., Blanco, L., and Salas, M. (1998) DNA polymerase template switching at specific sites on the phi 29 genome causes the in vivo accumulation of subgenomic phi 29 DNA molecules, *Mol. Microbiol. 29*, 787−798.
45. Anderson, J. A., Teufel, R. J., Yin, P. D., and Hu, W. S. (1998) Correlated template-switching events during minus-strand DNA synthesis: a mechanism for high negative interference during retroviral recombination, *J. Virol. 72*, 1186−1194.
46. Kao, C. C., Del Vecchio, A. M., and Zhong, W. (1999) De novo initiation of RNA synthesis by a recombinant flaviviridae RNA-dependent RNA polymerase, *Virology 253*, 1−7.
47. Arnold, J. J., and Cameron, C. E. (1999) Poliovirus RNA-dependent RNA polymerase (3D(pol)) is sufficient for template switching in vitro, *J. Biol. Chem. 274*, 2706−2716.
48. Kim, M. J., and Kao, C. (2001) Factors regulating template switch in vitro by viral RNA-dependent RNA polymerases: Implications for RNA-RNA recombination, *Proc. Natl. Acad. Sci. U.S.A. 98*, 4972−4977.
49. Hwang, S. B., Park, K. J., Kim, Y. S., Sung, Y. C., and Lai, M. M. (1997) Hepatitis C virus NS5B protein is a membrane-associated phosphoprotein with a predominantly perinuclear localization, *Virology 227*, 439−446.
50. Ferrari, E., Wright-Minogue, J., Fang, J. W., Baroudy, B. M., Lau, J. Y., and Hong, Z. (1999) Characterization of soluble hepatitis C virus RNA-dependent RNA polymerase expressed in *Escherichia coli*, *J. Virol. 73*, 1649−1654.

BI051483S